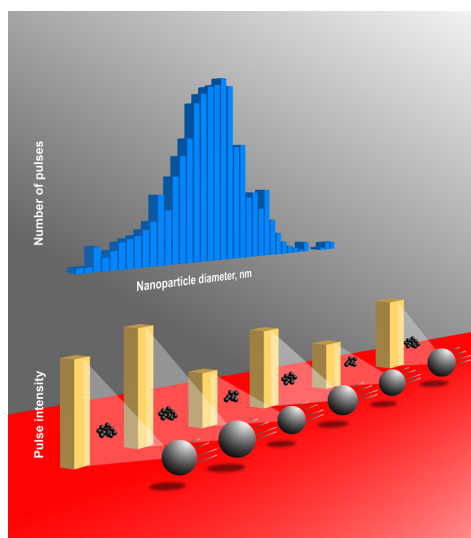


## Single Particle Inductively Coupled Plasma Mass Spectrometry: A Powerful Tool for Nanoanalysis

Single particle inductively coupled plasma mass spectrometry is an emergent ICPMS method for detecting, characterizing, and quantifying nanoparticles. Although the number of applications reported to date is limited, the relatively simple instrumental requirements, the low number concentration detection levels attainable, and the possibility to detect both the presence of dissolved and particulate forms of an element make this methodology very promising in the nanoscience related areas.

Francisco Laborda,\* Eduardo Bolea, and Javier Jiménez-Lamana

Group of Analytical Spectroscopy and Sensors, Institute of Environmental Sciences, University of Zaragoza, 50009 Zaragoza, Spain



F. Laborda

Single particle inductively coupled plasma mass spectrometry (SP-ICPMS) takes advantage of the well established elemental technique of ICPMS but performing measurements on a “particle by particle” basis. Single particle analysis using ICP optical emission spectrometry was first reported in 1986.<sup>1</sup> The methodology was initially adopted for analysis of aerosol and airborne particles<sup>1–5</sup> and suspensions of microparticles<sup>6</sup> and cells<sup>7</sup> being implemented in ICPMS instruments from 1993 to improve the attainable sensitivity of optical emission.<sup>8</sup> Afterward, the feasibility of SP-ICPMS for analysis of colloidal and microparticle suspensions was demonstrated by Degueldre et al. in a series of papers.<sup>9–13</sup> More recently, the rapid increase in the development, production, and use of engineered nanomaterials has led to renew the interest on single particle ICPMS as an alternative to other available techniques for detection, determination, and characterization of nanomaterials.<sup>14–16</sup>

Whereas nanomaterials are playing an increasing role in many fields, the knowledge about their potential impact on human health and the environment as well as the development of regulations and legislation for their control is being outpaced. It is recognized that innovative analytical approaches are

necessary for monitoring the presence of nanomaterials in environmental and biological media, assessing their potential impact and supporting regulations.<sup>17–19</sup> In this context, analytical chemistry is facing new challenges by regarding nanomaterials as analytes and not just as samples. In comparison with conventional analytes, the metrology of nanomaterials involves not only their detection and quantification but also their physicochemical characterization. One of the first challenges arises from the solid-state properties of nanomaterials. In addition to their chemical composition, a number of physical properties can be used for their characterization, which includes size, shape, surface charge, or surface area. Concentration levels are another critical challenge, which are especially significant when analyzing samples at environmentally relevant concentrations, where mass concentration detection limits below parts per billion should be achieved. Finally, these challenges have to be multiplied by the number of nanomaterials and the potential samples to be analyzed, which include from raw nanomaterials and industrial and consumer products to environmental and biological samples containing these nanomaterials.

Single particle ICPMS can be considered one of the innovative and emerging analytical approaches demanded by nanostakeholders. Although it is mainly used with suspensions of nanoparticles (NP), which are nanomaterials with all three external dimensions in the size range from 1 to 100 nm, it can be also applied to colloids and microparticles up to several micrometers as well as other nanomaterials with external dimensions in these ranges, like nanoplates and nanofibers.

Single particle ICPMS is able to provide information about the elemental chemical composition of noncarbon nanomaterials (carbon based nanomaterials are excluded due to the intrinsic low sensitivity of this element in ICPMS) as well as their number concentration, size, and the number size distribution. Because its dynamic range can be extended up to the micrometers region, polydispersed systems as well as aggregation or agglomeration processes may be studied. In addition, dissolved forms of the constituent elements of the nanoparticles can be detected and determined.<sup>15</sup> Finally, the low detection limits of ICPMS make single particle-ICPMS a

Published: December 5, 2013

suitable method for the analysis of environmental samples at environmentally relevant concentrations.

## ■ ICPMS AND NANOPARTICLES

ICPMS is considered one of the most versatile elemental techniques, providing rapid multielement analysis and low detection limits for a large range of samples on a routine basis. Although samples can be analyzed in any aggregation state, liquid is the most common. Liquid samples are introduced into the ICPMS instrument by using a nebulization system, consisting of a nebulizer and a spray chamber, which produces an aerosol of polydisperse droplets. Once the droplets are into the plasma, solvent evaporates, forming solid particles, which in turn are vaporized and their elements atomized and ionized. Ions are extracted through the interface into the mass spectrometer, where they are separated according to their mass/charge ratio and detected. Alternatively, suspensions can be introduced by using monodisperse droplet generators and in-house built introduction systems.<sup>20–23</sup>

Soluble forms of an element are distributed homogeneously within a solution, even at very low concentrations. Thus the mass of element entering the plasma per unit of time and traveling to the detector as ions can be considered constant, producing a “steady” signal during the reading period. By contrast, if the sample contains NPs, the element is no longer distributed homogeneously, being present as discrete groups of atoms. Then, if a sufficiently dilute suspension of NPs is nebulized into the plasma, a single pack of ions will be generated when each NP is vaporized, atomized, and ionized, which results in a transient signal of less than about 0.5 ms length.<sup>24</sup> Figure 1 shows the time-resolved signals of an element

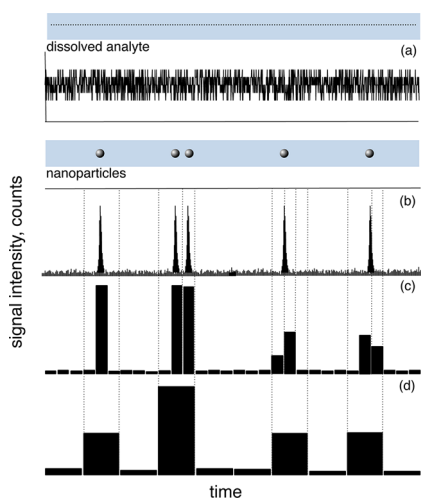


**Figure 1.** Time resolved ICPMS signals from a solution (a) and a nanoparticle suspension (b, c, and d) of the same element. Frequency of data acquisition: (a and b)  $\times 100$ , (c)  $\times 3$ , and (d)  $\times 1$  (not in scale).

being introduced into the ICPMS in dissolved form (part a) or as NPs (part b). From a quantitative point of view, particles with diameters below  $\sim 1 \mu\text{m}$  are completely vaporized in the time they spent in a plasma under standard conditions,<sup>24</sup> allowing the same sensitivity for suspensions or solutions of the same mass concentration.

Although NP suspensions behave and can be managed in ICPMS like conventional solutions, the measurement of individual NPs implies to record signals with respect to time

at high acquisition frequencies. By using fast data acquisition systems (greater than  $10^4$ – $10^5$  Hz), detailed information about the transient signal produced by each NP can be obtained (Figure 1b). However, commercial ICPMS instruments with quadrupole or single collector sector field mass spectrometers typically do not attain these high frequencies, and signals are measured as individual pulses with acquisition periods of one or more milliseconds, as it is shown in Figure 1c,d. These time scans are recorded during several seconds or minutes, and they consist of a number of spikes above a steady baseline, as it is shown in Figure 2a. Whereas each spike is due to the pack of ions from a NP, the baseline is due to the background or the presence of dissolved forms of the element measured. Raw time scans can be processed by plotting the signal intensity vs the signal intensity frequency, obtaining histograms as shown in Figure 2b, where the first distribution is due to the background and/or the presence of dissolved forms of the element measured and the second to the NPs.

## ■ BASIC PRINCIPLES

The basic assumption behind SP-ICPMS is that each recorded pulse represents a single NP. If this assumption is true then the frequency of the pulses is directly related to the number concentration of NPs and the intensity of each pulse is proportional to the mass of element, in fact to the number of atoms, in each detected NP. Theoretical basis of single particle detection applied to ICPMS were outlined by Degueldre et al.<sup>9–13</sup> for NP suspensions continuously introduced through conventional nebulization systems.

The relationship between the signal  $R$  (ions counted per time unit) and the mass concentration of a solution of an element  $M$  ( $C^M$ ), which is nebulized into an ICPMS, can be expressed as<sup>25</sup>

$$R = K_{\text{intro}} K_{\text{ICPMS}} K_M C^M \quad (1)$$

$K_{\text{intro}}$  ( $= \eta_{\text{nebul}} Q_{\text{sam}}$ ) represents the contribution from the sample introduction system, through the nebulization efficiency ( $\eta_{\text{nebul}}$ ) and the sample uptake rate ( $Q_{\text{sam}}$ ).  $K_{\text{ICPMS}}$  is the detection efficiency, which represents the ratio of the number of ions detected versus the number of atoms introduced into the ICP and involves the processes of ionization, sampling through the ICPMS interface, as well as the transmission through the mass spectrometer.  $K_M$  ( $= AN_{\text{Av}}/M_M$ ) includes the contribution from the element measured, where  $A$  is the atomic abundance of the isotope considered,  $N_{\text{Av}}$  the Avogadro number, and  $M_M$  the atomic mass of  $M$ .

For suspensions of spherical, solid, and pure NPs, the elemental mass concentration  $C_{\text{NP}}^M$  is expressed as

$$C_{\text{NP}}^M = \frac{4}{3} \pi \rho \left( \frac{d}{2} \right)^3 X_{\text{NP}} N_{\text{NP}} \quad (2)$$

where  $d$  is the NP diameter,  $\rho$  the density of the NPs,  $X_{\text{NP}}$  the mass fraction of the element in the NP (equal to 1 for a metallic NP), and  $N_{\text{NP}}$  the NP number concentration. Equation 1 can be adapted for the nebulization of this NP suspension as

$$R = K_{\text{intro}} K_{\text{ICPMS}} K_M K_{\text{NP}} N_{\text{NP}} \quad (3)$$

where  $K_{\text{NP}}$  ( $= 4/3 \pi \rho (d/2)^3 X_{\text{NP}}$ ) includes the properties of the NPs.

Single particle ICPMS involves the use of suspensions sufficiently diluted in order to detect just one NP per reading. Under such conditions, the flux of NPs reaching the plasma

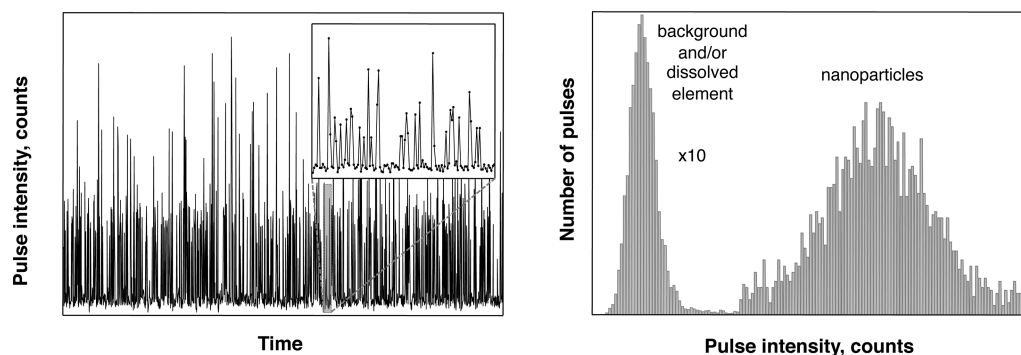


**Figure 2.** (a) Time scan of a nanoparticle suspension containing dissolved forms of the element contained in the nanoparticle. (b) Pulse intensity frequency histogram of data from part a.

( $Q_{\text{NP}}$ ) and hence the frequency of NPs detected ( $f_{\text{NP}}$ ) is given by the first contribution of eq 3, where

$$f_{\text{NP}} = Q_{\text{NP}} = \eta_{\text{neb}} Q_{\text{sam}} N_{\text{NP}} \quad (4)$$

When measurements are acquired in time-resolved mode, each reading lasts for a period equal to the dwell time ( $t_{\text{dwell}}$ ). Under such conditions, and if just one NP is detected during a single reading ( $\eta_{\text{neb}} Q_{\text{sam}} N_{\text{NP}} t_{\text{dwell}} = 1$ ),  $r_{\text{NP}}$  ( $= K_{\text{ICPMS}} K_{\text{M}} K_{\text{NP}}$ ) represents the total counts per reading and NP, which can be expressed with respect to the diameter of the NP as

$$r_{\text{NP}} = \frac{1}{6} \pi \rho X_{\text{NP}} K_{\text{ICPMS}} K_{\text{M}} d^3 \quad (5)$$

or to the mass of M per NP ( $m_{\text{NP}}$ ):

$$r_{\text{NP}} = K_{\text{ICPMS}} K_{\text{M}} m_{\text{NP}} \quad (6)$$

Equations 4–6 summarize the fundamentals behind single particle ICPMS. Quantitative determinations of NP number concentration are based on the linear relationship between the frequency of NP events and the number concentration (eq 4); whereas, the signal intensity of the NP events is proportional to the mass of analyte per NP (eq 6) or to the third power of the NP diameter for solid, spherical, and pure NPs (eq 5), allowing the determination of analyte mass per NP and size distributions, respectively.

## ■ PRACTICAL ASPECTS

When a NP suspension is introduced by conventional nebulization, NPs arrive in the plasma randomly and their flux must be low enough in order to obtain separate NP signals, as it is shown in Figure 1b. If acquisition frequencies of 1000 Hz or lower are used (dwell times of 1 ms or longer) the flux must be even lower to avoid the measurement of two or more NPs within a dwell time, as it is depicted in the second event of Figure 1d. Although the use of low dwell times (e.g., 1 ms) can be considered an useful option to prevent this problem, the risk of measuring a fraction of the whole signal is increased. These NPs partially detected are indistinguishable from the entire signal produced by a smaller NP, as it is shown in Figure 1c (NPs 4 and 5 starting from the left).

The probability of more than one NP being measured within a dwell time can be estimated by Poisson statistics.<sup>24</sup> Because this probability decreases with decreasing the dwell time and/or the flux of NPs, compromise conditions can be selected which guarantee the counting of an adequate number of one-NP events. In practice, dwell times between 3 and 10 ms are commonly used. Under such acquisition conditions, the NP

number concentration below  $10^8 \text{ L}^{-1}$  must be used to reduce the occurrence of two-NP events,<sup>15</sup> although this concentration depends in last instance on the nebulization system used, through its nebulization efficiency and the sample uptake rate (eq 4).

## ■ DETERMINATION OF NANOPARTICLE SIZE

In single particle analysis, the detection of NPs depends on two factors: (i) their number concentration, which should be high enough to allow counting a minimum number of events, and (ii) the size or the element mass per NP, which should be large enough to generate a pulse of ions detectable by the spectrometer.

If there is no limitation in the number of NPs, their detection is associated to the capability of identifying the pulses from the NPs over the baseline produced by the continuous background in a time scan like shown in Figure 2a. The smallest pulse height that can be distinguished from the background determines the smallest detectable NP mass that can be related to the smallest detectable NP size. Alternatively, NP pulses can be identified in a frequency histogram (Figure 2b) as events located at higher intensities than the background distribution. In any case, size detection limits ( $\text{LOD}_{\text{size}}$ ) can be established by<sup>25</sup>

$$\text{LOD}_{\text{size}} = \left( \frac{18\sigma_{\text{B}}}{\pi \rho X_{\text{NP}} K_{\text{ICPMS}} K_{\text{M}}} \right)^{1/3} \quad (7)$$

when a  $3\sigma$  criterion is used, where  $\sigma_{\text{B}}$  is the standard deviation of the continuous background.

Equation 7 shows that  $\text{LOD}_{\text{size}}$  depends basically on the detection efficiency. Thus, the improvement in the ionization conditions for elements with low ionization potentials as well as the increase on sampling or transmission of ions through more efficient instrumental designs can reduce the current size detection limits. Table 1 summarizes reported size and mass detection limits for metal and oxide based NPs. Metal NPs over  $\sim 20 \text{ nm}$  can be detected by SP-ICPMS, whereas the sizes increase for oxides, depending on their stoichiometry. With respect to mass, limits of detection are about tens of attograms per NP.

On the other hand, the upper size limit for particle characterization in SP-ICPMS is limited by the selective removal of large particles in the spray chamber<sup>26</sup> or their incomplete vaporization in the plasma.<sup>24</sup> In any case, 1–5  $\mu\text{m}$  are the maximum sizes recommended, which are sufficient for

**Table 1. Size and Element Mass Detection Limits Reported for Selected Nanoparticles Determined by SP-ICPMS**

nanoparticle	LOD <sub>size</sub>	LOD <sub>mass</sub>	ref
Ag	18 nm	32 ag	15
	<20 nm	<44 ag	20
	20 nm	44 ag	34,28
	33 nm	200 ag	21
	30 nm	535 ag	22
Au	21 nm	94 ag	21
	25 nm	158 ag	13
	17 nm	331 ag	22
U	10 nm	106 ag	22
Al <sub>2</sub> O <sub>3</sub>	30 nm	30 ag	9
ZrO <sub>2</sub>	70 nm	755 ag	10
ThO <sub>2</sub>	80 nm	2.4 fg	11
TiO <sub>2</sub>	100 nm	1.3 fg	9
FeOOH (goethite)	200 nm	10 fg	9

NPs and small aggregates characterization but may omit larger aggregates.

For elements which show significant contributions from plasma polyatomic ions (e.g., Si, Ti, Fe...) or from dissolved forms, both as part of the sample or as contamination, the magnitude of the continuous baseline affects negatively the size detection limits, through the background standard deviation ( $\sigma_B^2 = R_B t_{\text{dwell}}$ ). Thus, in such cases, the selection of longer dwell times involves an additional increase of size detection limits.<sup>27,28</sup>

For pure, solid, and spherical NPs, size information can be obtained by calibration with NP size standards of the same chemical composition by using eq 5. The logarithmic plot of the median pulse intensity for each NP standard versus its diameter provides a straight line with a slope close to 3,<sup>15</sup> as it is shown in Figure 3. Alternatively, these standards can be used to construct a mass calibration (eq 6) to obtain information about the mass per NP for heterogeneous NPs.

When size standards are not available, Pace et al.<sup>16</sup> have developed a procedure based on the use of dissolved standards of the element measured to determine the mass of analyte per NP and hence the NP diameter. The procedure, which is summarized in Figure 4, assumes that once in the plasma,

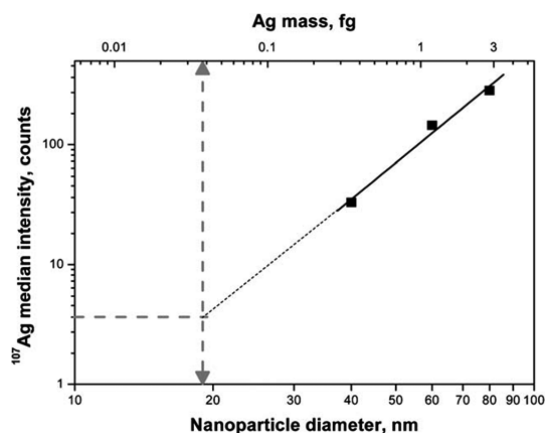


**Figure 3.** NP diameter/mass calibration vs <sup>107</sup>Ag pulse intensity. Gray dashed lines: limits of detection (3σ criterion). Reprinted with permission from ref 15. Copyright 2011 The Royal Society of Chemistry.

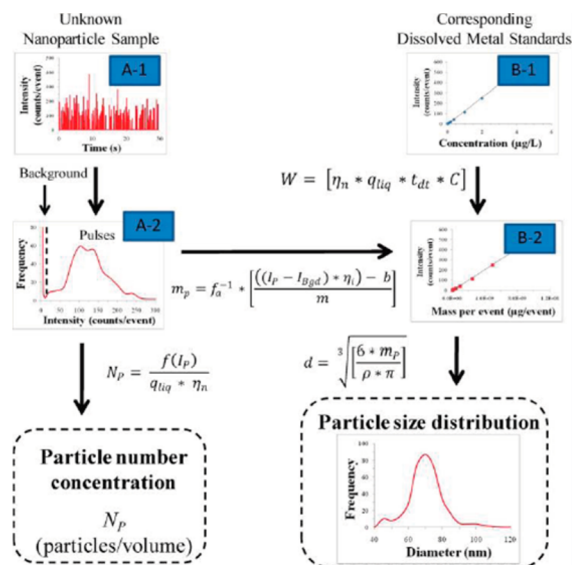


**Figure 4.** Data processing scheme for counting (path A) and sizing (paths A and B) nanoparticles using SP-ICPMS. (A-1) Raw data of unknown sample, (A-2) sorted and binned raw data to separate pulses from the background, (B-1) calibration curve of dissolved standards created for particle size calculation, (B-2) transformed calibration curve from concentration to mass per event. Reprinted from ref 16. Copyright 2011 American Chemical Society.

atoms from a dissolved standard solution and from a NP behave comparably for the same element. It involves knowing the nebulization efficiency, which is estimated by using a NP suspension of known number concentration, as the ratio of the detected NPs with respect to the calculated number of NPs nebulized.

## ■ QUANTIFICATION OF NANOPARTICLES: NUMBER CONCENTRATION

Working with NPs of detectable sizes, the frequency of NP events counted is directly related to the NP number concentration (eq 4). For a fixed NP number concentration ( $N_{\text{NP}}$ ), the number of events ( $N$ ) can be increased proportionally by increasing the total acquisition time ( $t_i$ ):

$$N = \eta_{\text{neb}} Q_{\text{sam}} t_i N_{\text{NP}} \quad (8)$$

The counting of NP events can be assimilated to an ideal Poisson counting process with zero blank, whose signal detection limit can be rounded to 3 counts. Thus the number concentration detection limit is associated to the capability of counting three NP events, which can be directly related to the number concentration limit of detection ( $\text{LOD}_{\text{NP}}$ ) through eq 8:

$$\text{LOD}_{\text{NP}} = 3 \times \frac{1}{\eta_{\text{neb}} Q_{\text{sam}} t_i} \quad (9)$$

Equation 9 shows that number concentration detection limits can be enhanced by improving nebulization efficiency, increasing the sample flow rate, and/or using longer acquisition times. In practice, NP detection limits in the range of  $10^6 \text{ L}^{-1}$  are reported with current ICPMS instruments.<sup>25,29</sup>

Number concentrations are independent of the NP nature, and calibrations are performed by using available number concentration standards. In practice, spherical solid and pure NP suspensions of known average diameter and mass



concentration (e.g., NIST RM 8013) are used for number concentration calibration, being suitable for the quantification of any type of suspension. Because the occurrence of two NP events increases at high number concentrations, the use of eq 8 should be limited to a maximum number concentration which guarantees the linear relationship between the number of events and the number concentration.<sup>25</sup>

### ■ DISSOLVED vs NANOPARTICLES

When a time scan is processed as a frequency distribution histogram (Figure 2b), specific information about the occurrence of dissolved and NP forms of the element measured can be obtained. If both distributions are fully resolved, the first one shows a Poisson profile, whereas the second one resembles the size distribution of the NPs, which tends to be log-normal.<sup>15</sup> When the distributions are not resolved, due to the high concentration of dissolved forms or the small size of the NPs, the Poisson distribution is lost and a tailed profile is obtained.<sup>15,25</sup>

Although the element mass concentration in a NP suspension can be determined by ICPMS working in standard mode, mass concentration can be determined in single particle mode by summing up the pulse intensity of the events recorded or by integrating the corresponding histograms (sum of the pulse intensities multiplied by the number of pulses, in Figure 2b). If such integration is performed for the different distributions obtained in the histograms, the content of the element as NPs and as dissolved forms can be obtained in terms of mass concentration if both distributions are fully resolved.

### ■ APPLICATIONS

Although SP-ICPMS is considered an emergent methodology yet, its current applications cover different fields: (i) detection and quantitation of NPs at environmental relevant concentrations, (ii) sizing and size distribution of nanomaterials, (iii) studies on stability of NPs, and (iv) migration and dissolution of NPs from solid matrixes.

**Detection and Quantitation of Nanoparticles in Environmental Samples.** The capability of SP-ICPMS for detection of NPs in environmental samples has been tested by the analysis of wastewaters from treatment plants.<sup>28,30</sup> Mitrano et al.<sup>30</sup> detected and quantified both dissolved and nanoparticulated silver at the  $\text{ng L}^{-1}$  level in influent and effluent samples from a wastewater treatment plant. Figure 5 shows SP-ICPMS time scans that confirm the presence of dissolved as well as particulate silver in the wastewater samples. Tuoriniemi et al.<sup>28</sup> detected NPs containing silver, cerium, and titanium in wastewater effluent samples at concentrations of 2000–30 000  $\text{mL}^{-1}$ , which were in agreement with predicted concentrations in Europe, although the specific nature of the particles was not determined.

As a consequence of the use of consumer products containing NPs, they can be released into the environment. Thus silver NPs were detected in the effluent of a commercially available nanosilver washing machine by SP-ICPMS.<sup>31</sup> The concentration of silver containing particles was determined to be  $\sim 10^8$  particles  $\text{mL}^{-1}$ . The majority of the silver NPs were below 20 nm; however, a small amount of larger particles was also present in the effluent. Because of the low number concentration detection limits of SP-ICPMS, Coleman et al.<sup>32</sup>

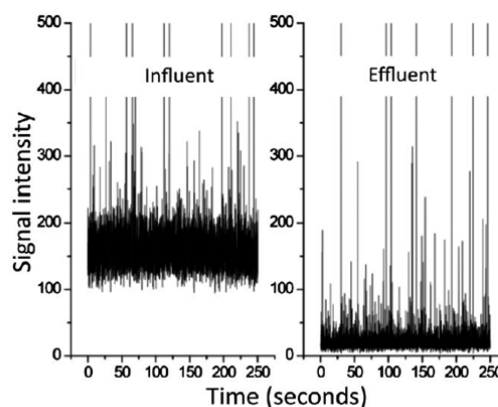


**Figure 5.** Evidence of dissolved silver (elevated continuous background) and nanoparticulate silver (pulses) in wastewater measured by SP-ICPMS. Reprinted with permission from ref 30. Copyright 2012 Wiley.

were able to detect the retention of NPs in invertebrates *Lumbriculus variegatus* exposed to 70 nm silver NPs.

Although carbon-based NPs cannot be detected directly by SP-ICPMS, Reed et al.<sup>33</sup> have used the residual catalyst metals (cobalt, yttrium, molybdenum, nickel) contained in carbon nanotubes for their detection at  $\text{ng L}^{-1}$  levels. In spite of quantitative results that could not be obtained, the method allowed one to screen the release of carbon nanotubes from a polymeric matrix.

**Sizing and Size Distribution of Nanomaterials.** Pace et al.<sup>34</sup> have shown that SP-ICPMS is able to size silver NPs, across different sizes and number concentrations, with accuracy similar to other commercially available techniques, namely, dynamic light scattering (DLS), differential centrifugal sedimentation (DCS), nanoparticle tracking analysis (NTA), and transmission electron microscopy (TEM).

Loeschner et al.<sup>35</sup> have used ICPMS in single particle mode to obtain the number size distribution of silver NPs in meat digestates. When compared to TEM, some differences were observed for the size distributions although similar results were obtained for the maxima, as it can be shown in Figure 6. These differences arose from the size detection limit attained by SP-ICPMS that hindered the detection of NPs smaller than 15 nm. Also the fact that just the diameters of the primary particles were measured by TEM, whereas aggregates/agglomerates were also measured by SP-ICPMS, can justify them.

The European Commission (EC) published in 2011 a definition of the term “nanomaterial” for regulatory purposes based on the size of the NPs and their number size distribution.<sup>36</sup> In this respect, a report by the Institute of Reference Materials and Measurements of the EC,<sup>37</sup> related to the requirements on measurements for the implementation of this definition, included SP-ICPMS in addition to other current available methods due to its intrinsic potential. Recently, Laborda et al. have applied SP-ICPMS to estimate the number size distribution of different commercial nanomaterials in the context of the EC definition with successful results.<sup>25</sup>

**Stability of Nanoparticles.** NPs can undergo a number of transformations under biological or environmental conditions. Primary NPs can form agglomerates or aggregates of bigger sizes, being reversible just in the first case. On the other hand, some metal-containing NPs (silver, zinc oxide) can dissolve, releasing soluble species. As we have stated throughout the paper, SP-ICPMS is capable of handling NPs as well as their

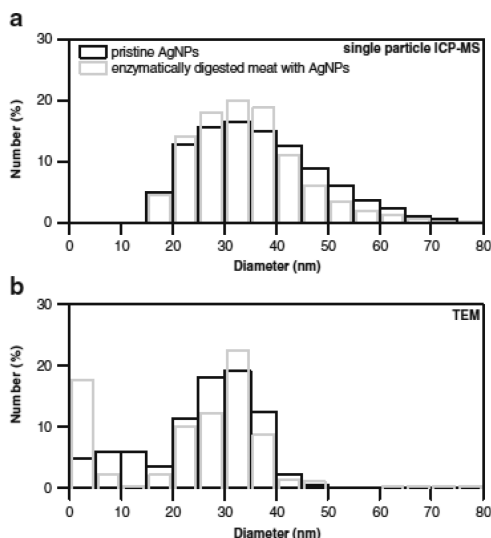


**Figure 6.** Normalized number size distributions based on (a) SP-ICPMS and (b) TEM for the pristine silver nanoparticles and for silver nanoparticles in meat after enzymatic digestion. Reprinted with permission from ref 35. Copyright 2013 Springer.

transformation products, both as aggregates and dissolved forms. Following this trend, SP-ICPMS has been used for quantitation of dissolved silver from silver NPs under laboratory conditions.<sup>38</sup>

The stability of silver NPs in algal growth medium has been studied by Pace et al.<sup>34</sup> In Figure 7 it can be observed that the

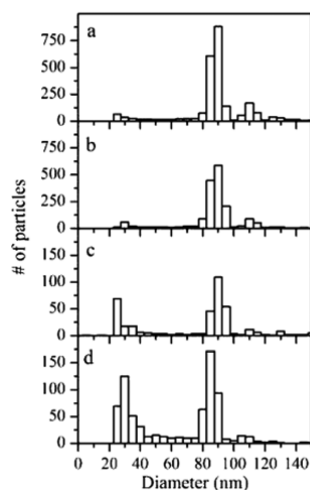


**Figure 7.** Nanoparticle size distribution of 100 nm silver nanoparticles in algal growth medium before and after incubation at different silver concentrations: (a) at 0 h, (b) after 144 h at  $1000 \mu\text{g L}^{-1}$ , (c) after 144 h at  $50 \mu\text{g L}^{-1}$ , and (d) after 144 h at  $6 \mu\text{g L}^{-1}$ . Reprinted from ref 34. Copyright 2012 American Chemical Society.

appearance of a secondary distribution at sizes lower than the original one after incubation, what was hypothesized as being due to formation of silver chloride after oxidation of silver NPs.

By using SP-ICPMS in combination with DLS and SEM, Walczak et al.<sup>39</sup> have studied the fate of silver NPs during gastrointestinal digestion. The study concluded that after gastric digestion, the number of NPs dropped significantly due to the formation of clusters composed of primary silver NPs and chlorine (not observed by SP-ICPMS), but it rose back to

original values after the intestinal digestion and disagglomeration of the clusters.

**Migration and Dissolution of Nanoparticles from Solid Matrixes.** SP-ICPMS has been applied in studies on the releasing and dissolution of silver NPs from plastic food storage containers.<sup>40,41</sup> Although the methodology has not been fully exploited, it has allowed to distinguish the presence of NPs from dissolved silver in different food simulants (water, ethanol, acetic acid) used in the migration studies as well as the relative mass distribution of both silver forms.

## ■ COUPLING OF SP-ICPMS TO SIZE SEPARATION TECHNIQUES

In last instance, SP-ICPMS is just able of measuring the elements present in a particle. This means that two different NPs with the same element content behave in SP-ICPMS in the same way. This can be the case for NPs of different shapes or NPs with the same shape and core diameter but showing different coatings. Transmission electron microscopy can provide information about the shape of inorganic NPs, in order to convert the mass per NP information obtained by SP-ICPMS into size/diameter information. However, for inorganic NPs coated with an organic moiety, other suitable techniques for providing the size of the actual NP are needed.

Field flow fractionation (FFF) and hydrodynamic chromatography (HDC) are two separation techniques which separates particles according to their hydrodynamic diameter. These techniques, when coupled to SP-ICPMS can provide an additional selectivity that SP-ICPMS lacks.<sup>42</sup> Up until now, just HDC has been coupled online to SP-ICPMS, confirming the potential of this approach.<sup>43</sup> Figure 8 shows the three-

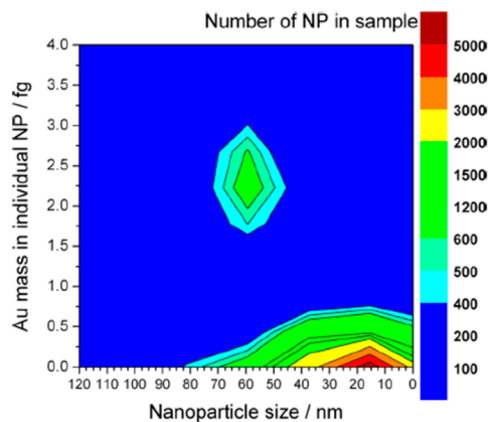


**Figure 8.** Three-dimensional hydrodynamic chromatogram obtained from 30 and 60 nm gold nanoparticles detected online by ICPMS in single detection mode. The chromatogram provides information about number concentration, metal content per nanoparticle, and nanoparticle diameters. Reprinted from ref 43. Copyright 2012 American Chemical Society.

dimensional chromatogram obtained by HDC-SP-ICPMS, which provides information about the number concentration and metal content of NPs as well as about their size. Despite that the coupled technique has just been applied to pure gold NPs, it is suitable of being used with heterogeneous NPs of different nature.

Although FFF has not been coupled online to SP-ICPMS, Loeschner et al.<sup>35</sup> have measured fractions collected from separations performed by asymmetric flow field flow fractiona-

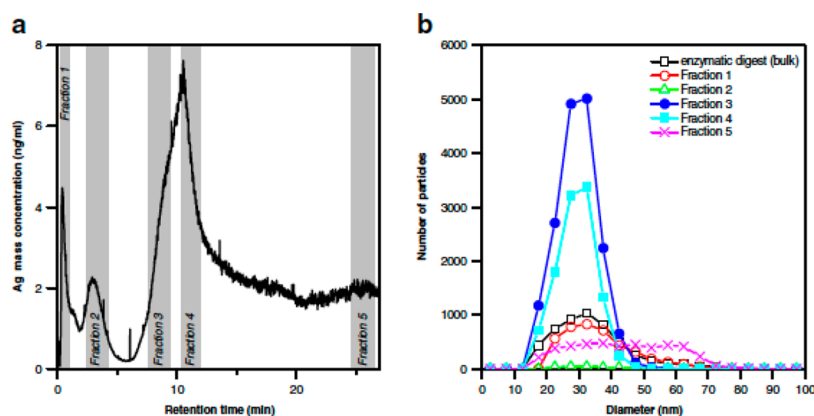


**Figure 9.** (a) AsFIFFF-ICPMS fractogram of an enzymatically digested meat sample containing silver nanoparticles and fractions collected for offline SP-ICPMS analysis. (b) Number size distributions for all fractions and for the enzymatic digested (bulk) sample. Reprinted with permission from ref 35. Copyright 2013 Springer.

**Table 2. Analytical Information Available from Samples Containing Dissolved and Nanoparticle Forms of an Element Analyzed by SP-ICPMS**

	analytical information	signal	units	standards
detection	dissolved nanoparticle	histogram distribution (no. events vs pulse intensity)		none
characterization	dissolved + nanoparticle			
	elemental composition	pulse intensity		none
	mass distribution mean mass per nanoparticle	histogram distribution (no. events vs mass)	fg	nanoparticles (mass) or dissolved standard
	size distribution mean diameter	histogram distribution (no. events vs diameter)	nm	nanoparticles (diameter) or dissolved standard
quantitation	nanoparticle number concentration	number of events per distribution	L <sup>-1</sup>	nanoparticles (diameter and mass concentration)
	element mass concentration	number of events × pulse intensity per event	ng L <sup>-1</sup>	dissolved standard

tion by SP-ICPMS (offline coupling AsFIFFF–SP-ICPMS). In this work, selected fractions from enzymatically digested meat samples spiked with silver NPs were measured by ICPMS in single particle mode to obtain the corresponding number size distributions and to detect the occurrence of dissolved silver, as it is shown in Figure 9.

Ion-mobility spectrometry (IMS) is a separation technique based on a combination of mass, charge, size, and shape of previously ionized species. The technique has been used with success for the analysis of nanosize species such as macromolecules, viruses, and NPs by using condensation particle counting detectors. Recently, nanoelectrospray IMS has been offline coupled to an ICPMS operating in single particle mode,<sup>44</sup> demonstrating the feasibility of the hyphenated technique for element-specific size determination of gold NPs.

## ■ LIMITATIONS AND FURTHER INSTRUMENTAL DEVELOPMENTS

As previously stated, the signal produced by a single NP in SP-ICPMS is proportional to the mass of the element in the NP. This means that the composition, density, and shape of the NP must be known to get information about its size. Thus combination of SP-ICPMS with imaging techniques, like electron or atomic force microscopy, is recommended.

At present, SP-ICPMS is particularly suitable for NPs consisting of one element only and sizes higher than ~20 nm. In order to enhance size detection limits and implement multielement capabilities for heterogeneous NPs, improved commercially available ICPMS instruments are needed.

With respect to improving size detection limits, eq 7 shows that the detection of smaller sized NPs involves the use of ICPMS instruments with higher detection efficiency (ratio of ions detected per NP vs atoms per NP). Detection efficiencies of current quadrupole instruments are around 10<sup>-6</sup> counts per atom,<sup>21</sup> although detection efficiencies of 10<sup>-4</sup> counts per atom have been reported by introducing desolvated aerosols.<sup>20</sup> In any case, reducing size detection limits down to the 1-nm range requires ICPMS instruments with detection efficiencies around 10<sup>-3</sup> counts per atom.

Because the duration of the transient signal generated by an individual NP is in the range of hundreds of microseconds, the multielement detection of transient signal generated by individual NPs involves the use of simultaneous or fast scanning instruments, able of recording full spectra of a mass range of interest at frequencies around 10<sup>5</sup> Hz.<sup>45</sup> Apart from specialized multicollector ICPMS instruments, other commercially available options for simultaneous multielement detection would be time-of-flight spectrometers (TOF-ICPMS) and double focusing sector field instruments equipped with array detectors. However, the currently available instruments do not permit the continuous monitoring at acquisition times below several tens of milliseconds,<sup>22</sup> being useless for multielement SP-ICPMS. Recently, Borovinskaya et al. have developed a prototype TOF-ICPMS capable of quasi-simultaneous multielement detection at acquisition times of 33 μs and with detection efficiencies similar to those of quadrupole-based instruments.<sup>22</sup>



Quadrupole and single collector sector field instruments, working in single particle mode, are usually limited to monitor just one isotope due to the sequential scanning nature of these mass analyzers. However, fast scanning modes have recently been proposed both for sector field<sup>46</sup> and quadrupole instruments.<sup>47</sup> An acquisition frequency of  $10^4$  Hz (acquisition time of 100  $\mu$ s) has been reported using a sector field ICPMS, whereas  $10^6$  Hz has been attained with a commercial quadrupole, which involves acquisition times down to 1  $\mu$ s. Nevertheless, attainable settling times between isotopes can be a limitation for multielement detection in a single nanoparticle.

Liquid sample introduction in commercial ICPMS instrument is based on the use of pneumatic nebulization systems, which involve the random arrival of polydisperse aerosol droplets into the plasma. Alternatively, monodisperse droplet generators have been used for introduction of NP suspensions in single particle mode.<sup>20–23</sup> These generators are able to produce pulsed microdroplets at adjustable frequency (up to 100 Hz) and droplet size (below 100  $\mu$ m) and are coupled to custom-built delivery systems for transport of the droplets to the plasma. These systems provide nebulization efficiencies higher than 95%, although at extremely low sample flow rates. Their main feature is the possibility of performing size/mass calibrations just by using dissolved standards and knowing the diameter of the droplets.<sup>21,23</sup>

## CONCLUSIONS

Table 2 summarizes the different types of information that can be obtained from SP-ICPMS. By analyzing a sample in an ICPMS running in single particle mode it is possible to detect both the presence of dissolved and particulate forms of an element, to determine their respective mass concentrations, as well as the number concentration of NPs. With respect to characterization, size information about the average diameter and the size distribution can be obtained if additional information about shape and composition is known, otherwise information about the mass of element per NP will be attained. Lastly, ICPMS also provides chemical information about the elemental composition of the nanomaterial analyzed, in contrast to other techniques like DLS, NTA, or DCS.

Undoubtedly, the main feature of SP-ICPMS is that all the information summarized in Table 2 is available by using commercial ICPMS instruments, which makes the methodology easily accessible to any ICPMS user. In this regard, SP-ICPMS is on its way to expand out from the research laboratories. By way of example, ICPMS manufacturers are becoming aware of the capability of SP-ICPMS<sup>48</sup> and some of them have already launched application notes for spreading this methodology.<sup>49,50</sup>

## AUTHOR INFORMATION

### Corresponding Author

\*E-mail: flaborda@unizar.es.

### Notes

The authors declare no competing financial interest.

### Biography

Dr. Francisco Laborda is Professor of Analytical Chemistry at the University of Zaragoza. His research focuses on the development of novel approaches for physicochemical elemental speciation, with special attention to single detection ICPMS and separation techniques hyphenated to ICPMS and their application to analytes in the nanometer–micrometer range for environmental and nanomaterial

analysis. Dr. Eduardo Bolea is Associate Professor in the Department of Analytical Chemistry at the University of Zaragoza. His research focuses on the development of methods for the detection, characterization, and quantitation of analytes in the range of nanometers, based on field flow fractionation techniques and single particle ICPMS. Dr. Laborda and Dr. Bolea belong to the Group of Analytical Spectroscopy and Sensors (GEAS) of the Institute of Environmental Sciences (IUCA) at the University of Zaragoza. Javier Jiménez-Lamana is a Ph.D. student in the Group of Analytical Spectroscopy and Sensors. With a B.Sc. in Chemistry from the University of Zaragoza, his research focuses on developing analytical methods for the analysis of nanomaterials.

## ACKNOWLEDGMENTS

The authors gratefully acknowledge support from the Spanish Ministry of Economy and Competitiveness (Project CTQ2012-38091-C02-01).

## REFERENCES

- (1) Kawaguchi, H.; Fukusawa, N.; Mizuike, A. *Spectrochim. Acta, Part B* **1986**, *41*, 1277–1286.
- (2) Kawaguchi, H.; Kamakura, K.; Maeda, E.; Mizuike, A. *Bunseki Kagaku* **1987**, *36*, 431–435.
- (3) Nomizu, T.; Nakashima, H.; Hotta, Y.; Tanaka, T.; Kawaguchi, H. *Anal. Sci.* **1992**, *8*, 527–531.
- (4) Bochert, U. K.; Dannecker, W. *J. Aerosol Sci.* **1989**, *20*, 1525–1528.
- (5) Bochert, U. K.; Dannecker, W. *J. Aerosol Sci.* **1992**, *23*, S417–S420.
- (6) Garcia, C. C.; Murtazin, A.; Groh, S.; Horvatic, V.; Niemax, K. *J. Anal. At. Spectrom.* **2010**, *25*, 645–653.
- (7) Nomizu, T.; Kaneco, S.; Tanaka, T.; Ito, D.; Kawaguchi, H.; Vallee, B. T. *Anal. Chem.* **1994**, *66*, 3000–3004.
- (8) Kawaguchi, H.; Tanaka, T. *Anal. Sci.* **1993**, *9*, 843–846.
- (9) Degueldre, C.; Favarger, P.-Y. *Colloids Surf., A* **2003**, *217*, 137–142.
- (10) Degueldre, C.; Favarger, P.-Y.; Bitea, C. *Anal. Chim. Acta* **2004**, *518*, 137–142.
- (11) Degueldre, C.; Favarger, P.-Y. *Talanta* **2004**, *62*, 1051–1054.
- (12) Degueldre, C.; Favarger, P.-Y.; Rossé, R.; Wold, S. *Talanta* **2006**, *68*, 623–628.
- (13) Degueldre, C.; Favarger, P.; Wold, S. *Anal. Chim. Acta* **2006**, *555*, 263–268.
- (14) Heithmar, E. M.; Pergantis, S. A. *Characterizing Concentrations and Size Distributions of Metal-containing Nanoparticles in Waste Water*, EPA/600/R-10/117, U.S. Environmental Protection Agency, 2010.
- (15) Laborda, F.; Jiménez-Lamana, J.; Bolea, E.; Castillo, J. R. *J. Anal. At. Spectrom.* **2011**, *26*, 1362–1371.
- (16) Pace, H. E.; Rogers, N. J.; Jarolimek, C.; Coleman, V. A.; Higgins, C. P.; Ranville, J. F. *Anal. Chem.* **2011**, *83*, 9361–9369.
- (17) Klaine, S. J.; Alvarez, P. J. J.; Batley, G. E.; Fernandes, T. F.; Handy, R. D.; Lyon, D. Y.; Mahendra, S.; McLaughlin, M. J.; Lead, J. R. *Environ. Toxicol. Chem.* **2008**, *27*, 1825–1851.
- (18) Baun, A.; Hartmann, N. B.; Grieger, K. D.; Foss Hansen, S. *J. Environ. Monit.* **2009**, *11*, 1774–1781.
- (19) Howard, A. G. *J. Environ. Monit.* **2010**, *12*, 135–142.
- (20) Franze, B.; Strenge, I.; Engelhard, C. *J. Anal. At. Spectrom.* **2012**, *27*, 1074–1083.
- (21) Gschwind, S.; Flamigni, L.; Koch, J.; Borovinskaya, O.; Groh, S.; Niemax, K.; Günther, D. *J. Anal. At. Spectrom.* **2011**, *26*, 1166–1174.
- (22) Borovinskaya, O.; Hattendorf, B.; Tanner, M.; Gschwind, S.; Günther, D. *J. Anal. At. Spectrom.* **2013**, *28*, 226–233.
- (23) Gschwind, S.; Hagendorfer, H.; Frick, D. A.; Günther, D. *Anal. Chem.* **2013**, *85*, 5875–5883.
- (24) Olesik, J. W.; Gray, P. J. *J. Anal. At. Spectrom.* **2012**, *27*, 1143–1155.



- (25) Laborda, F.; Jimenez-Lamana, J.; Bolea, E.; Castillo, J. R. *J. Anal. At. Spectrom.* **2013**, *28*, 1220–1232.
- (26) Goodall, P.; Foulkes, M. E.; Ebdon, L. *Spectrochim. Acta, Part B* **1993**, *48*, 1563–1577.
- (27) Reed, R. B.; Higgins, C. P.; Westerhoff, P.; Tadjiki, S.; Ranville, J. F. *J. Anal. At. Spectrom.* **2012**, *27*, 1093–1100.
- (28) Tuoriniemi, J.; Cornelis, G.; Hassellöv, M. *Anal. Chem.* **2012**, *84*, 3965–3972.
- (29) Mitrano, D. M.; Barber, A.; Bednar, A.; Westerhoff, P.; Higgins, C. P.; Ranville, J. F. *J. Anal. At. Spectrom.* **2012**, *27*, 1131–1142.
- (30) Mitrano, D. M.; Leshner, E. K.; Bednar, A.; Monsrud, J.; Higgins, C. P.; Ranville, J. F. *Environ. Toxicol. Chem.* **2012**, *31*, 115–121.
- (31) Farkas, J.; Peter, H.; Christian, P.; Gallego Urrea, J. A.; Hassellöv, M.; Tuoriniemi, J.; Gustafsson, S.; Olsson, E.; Hylland, K.; Thomas, K. V. *Environ. Int.* **2011**, *37*, 1057–1062.
- (32) Coleman, J. G.; Kennedy, A. J.; Bednar, A. J.; Ranville, J. F.; Laird, J. G.; Harmon, A. R.; Hayes, C. A.; Gray, E. P.; Higgins, C. P.; Lotufo, G.; Steevens, J. A. *Environ. Toxicol. Chem.* **2013**, *32*, 2069–2077.
- (33) Reed, R. B.; Goodwin, D. G.; Marsh, K. L.; Capracotta, S. S.; Higgins, C. P.; Fairbrother, D. H.; Ranville, J. F. *Environ. Sci.: Processes Impacts* **2013**, *15*, 204–213.
- (34) Pace, H. E.; Rogers, N. J.; Jarolimek, C.; Coleman, V. A.; Gray, E. P.; Higgins, C. P.; Ranville, J. F. *Environ. Sci. Technol.* **2012**, *46*, 12272–12280.
- (35) Loeschner, K.; Navratilova, J.; Købler, C.; Mølhave, K.; Wagner, S.; von der Kammer, F.; Larsen, E. H. *Anal. Bioanal. Chem.* **2013**, *405*, 8185–8195.
- (36) European Commission. 2011/696/EU: Commission Recommendation of 18 October 2011 on the definition of nanomaterial. *Off. J. Eur. Commission* **2011**, *275*, 38–40.
- (37) Lisinger, T.; Roebben, G.; Gilliland, D.; Calzolari, L.; Rossi, F.; Gibson, N.; Klein, C. *Requirements on measurements for the implementation of the European Commission definition of the term "nanomaterial"*; Joint Research Centre, Institute for Reference Materials and Measurements. Publication Office of the European Union: Luxembourg, 2012.
- (38) Hadioui, M.; Leclerc, S.; Wilkinson, K. J. *Talanta* **2013**, *105*, 15–19.
- (39) Walczak, A. P.; Fokkink, R.; Peters, R.; Tromp, P.; Herrera Rivera, Z. E.; Rietjens, I. M. C. M.; Hendriksen, P. J. M.; Bouwmeester, H. *Nanotoxicology* **2013**, *7*, 1198–1210.
- (40) Goetz, N.; von Fabricius, L.; Glaus, R.; Weitbrecht, V.; Günther, D.; Hungerbühler, K. *Food Addit. Contam., Part A* **2013**, *30*, 612–620.
- (41) Echegoyen, Y.; Nerin, C. *Food Chem. Toxicol.* **2013**, *62*, 16–22.
- (42) Kammer, F.; von der Ferguson, P. L.; Holden, P.; Masion, A.; Rogers, K. R.; Klaine, S. J.; Koelmans, A.; Horne, N.; Unrine, J. M. *Environ. Toxicol. Chem.* **2012**, *31*, 32–49.
- (43) Pergantis, S. A.; Jones-Lepp, T. L.; Heithmar, E. M. *Anal. Chem.* **2012**, *84*, 6454–6462.
- (44) Kapellios, E. A.; Pergantis, S. A. *J. Anal. At. Spectrom.* **2012**, *27*, 21–24.
- (45) Engelhard, C. *Anal. Bioanal. Chem.* **2011**, *399*, 213–219.
- (46) Shigeta, K.; Koellensperger, G.; Rampler, E.; Traub, H.; Rottmann, L.; Panne, U.; Okino, A.; Jakubowski, N. *J. Anal. At. Spectrom.* **2013**, *28*, 637–645.
- (47) Badiei, H.; Kajen, K. Single particle analysis using ultra-fast quadrupole ICP-MS. *European Winter Conference in Plasma Spectrometry*, Krakow, Poland, 2013.
- (48) Salamon, A. W. *Environ. Eng. Sci.* **2013**, *30*, 101–108.
- (49) Stephan, C.; Hineman, A. *Analysis of NIST Gold Nanoparticles Reference Materials Using the NexION 300 ICP-MS in Single Particle Mode*; Application Note, Perkin Elmer, Inc., 2012.
- (50) Sannac, S.; Tadjiki, S.; Moldenhauer, E. *Single particle analysis using the Agilent 7700x ICP-MS*; Application Note 5991-2929EN, Agilent Technologies, Inc., 2013.